

Abrupt change in the energy gap of superconducting $\text{Ba}_{1-x}\text{K}_x\text{Fe}_2\text{As}_2$ single crystals with hole doping

W. Malaeb,^{1,2} T. Shimojima,^{1,3} Y. Ishida,^{1,3} K. Okazaki,^{1,3} Y. Ota,¹ K. Ohgushi,^{1,2}
K. Kihou,^{2,4} T. Saito,⁵ C.H. Lee,^{2,4} S. Ishida,^{4,6} M. Nakajima,^{4,6} S. Uchida,⁶ H. Fukazawa,^{2,5}
Y. Kohori,^{2,5} A. Iyo,^{2,4} H. Eisaki,^{2,4} C.-T. Chen,⁷ S. Watanabe,¹ H. Ikeda,⁸ and S. Shin^{1,2,3}

¹*Institute for Solid State Physics (ISSP), University of Tokyo,
Kashiwa-no-ha, Kashiwa, Chiba 277-8561, Japan*

²*TRIP, JST, Chiyoda-ku, Tokyo 102-0075, Japan*

³*CREST, JST, Chiyoda-ku, Tokyo 102-0075, Japan*

⁴*National Institute of Advanced Industrial Science and Technology (AIST), Tsukuba, Ibaraki 305-8568, Japan*

⁵*Department of Physics, Chiba University, Chiba 263-8522, Japan*

⁶*Department of Physics, University of Tokyo, Tokyo 113-8656, Japan*

⁷*Beijing Center for Crystal R and D, Chinese Academy of Science (CAS), Zhongguancun, Beijing 100190, China*

⁸*Department of Physics, Kyoto University, Sakyo-ku, Kyoto 606-8502, Japan*

(Dated: November 5, 2018)

We performed a Laser angle-resolved photoemission spectroscopy (ARPES) study on a wide doping range of $\text{Ba}_{1-x}\text{K}_x\text{Fe}_2\text{As}_2$ (BaK) and precisely determined the doping evolution of the superconducting (SC) gaps in this compound. The gap size of the outer hole Fermi surface (FS) sheet around the Brillouin zone (BZ) center shows an abrupt drop with overdoping (for $x \gtrsim 0.6$) while the inner and middle FS gaps roughly scale with T_c . This is accompanied by the simultaneous disappearance of the electron FS sheet with similar orbital character at the BZ corner. These results browse the different contributions of $X^2 - Y^2$ and XZ/YZ orbitals to superconductivity in BaK and can be hardly completely reproduced by the available theories on iron-based superconductors.

A detailed knowledge of the superconducting (SC) gap size and anisotropy is essential for understanding the electron pairing mechanism in iron pnictides [1]. From the early stage, it was thought that electron pairing is likely to be of magnetic origin induced by antiferromagnetic (AFM) spin-fluctuations (SF) between disconnected Fermi surface (FS) sheets [2–4]. Within this interband scattering picture, a full sign-reversing superconducting (SC) gap (s^{+-}) is expected which was supported by the findings of angle-resolved photoemission spectroscopy (ARPES) studies [5–8] and other experimental results [9–11]. However, some theoretical studies [12–14] have pointed out to a possible role of the orbital degrees of freedom in the pairing mechanism. This was supported by a recent Laser ARPES study on SC $\text{BaFe}_2(\text{As}_{1-x}\text{P}_x)_2$ (AsP) and optimally-doped (OP) $\text{Ba}_{1-x}\text{K}_x\text{Fe}_2\text{As}_2$ (BaK) compounds [15] which found nearly orbital-independent SC gaps on the hole-like FS sheets around the Brillouin Zone (BZ) center. Nevertheless, there is an increasing evidence that the SC gap in iron pnictides is not universal [16], as there is evidence for gap nodes in some compounds such as in AsP [16–18], KFe_2As_2 [19–21] and $\text{Ba}(\text{Fe}_{1-x}\text{Co}_x)_2\text{As}_2$ [22].

Among other iron pnictides, BaK is special regarding the persistence of superconductivity in this compound up to the end member KFe_2As_2 . Also the SC gaps in BaK are expected to change with doping from fully-opened gaps near the OP region [5–7] to nodal gaps at the end member KFe_2As_2 [19–21]. Therefore, BaK is an ideal system to study the doping evolution of SC gaps. Moreover, it is important to investigate the significance of each orbital component to the unconventional pairing mechanism in BaK and its doping evolution which will be a

crucial test for the validity of available theories on iron pnictides. While ARPES is the most direct experimental technique in probing the electronic structure of solids and addressing the above issues, there is still little consensus on the SC gaps of iron pnictides, including BaK, determined from ARPES. Indeed, part of this originates from the limited experimental resolution. Here, we have implemented Laser ARPES with high energy resolution and bulk sensitivity on a wide doping range of BaK extending from the underdoped (UD) to the overdoped (OD) regime. This enabled the assignment of the orbital character of each of the hole bands around the BZ center and the precise determination of the doping evolution of the SC gaps on each of these bands.

High-quality single crystals of underdoped (UD) ($x \sim 0.2, 0.3$) and overdoped (OD) ($x \sim 0.5, 0.6, 0.7$ and 0.85) $\text{Ba}_{1-x}\text{K}_x\text{Fe}_2\text{As}_2$ (BaK) were grown by using the FeAs [23] and KAs [24] flux respectively. Laser ARPES measurements were carried out at ISSP, University of Tokyo. We used a VG-Scienta R4000 as an electron analyzer and a VUV Laser of $h\nu = 6.994$ eV as a light source. In this spectrometer [25], changing the polarization vector of the laser source is possible by rotating the half-wave ($\lambda/2$) plate without changing the optical path. The Fermi level (E_F) calibration of the samples was done by referring to that of gold and the energy resolution was set to ~ 3 meV. The samples were cleaved at a temperature $T \sim 30$ K or less in an ultra-high vacuum of less than 5×10^{-11} Torr. Other ARPES measurements were performed using a Helium discharge source with $h\nu = 21.218$ eV. In this case, the electron analyzer is similar to that of the Laser spectrometer. Also the sample cleaving and E_F calibration are similar to the Laser ARPES case, however the energy

resolution in this case was set to ~ 10 meV.

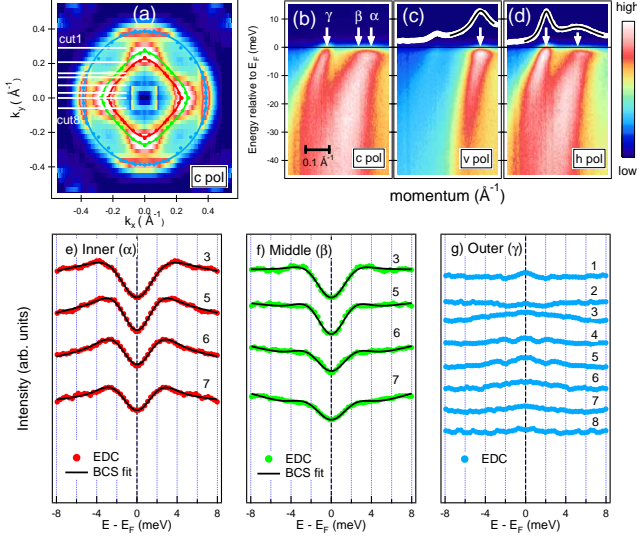


FIG. 1: (color online) Laser ARPES data of heavily OD BaK ($x \sim 0.7$, $T_c \sim 20$ K): (a) FS map in the k_x - k_y plane measured at $T \sim 7$ K with circularly-polarized light. The intensity was integrated within a window of ± 5 meV around E_F and four-fold symmetrization was done. The dots indicate the k_F points determined from MDCs fitting and the colored curves are guides to the eye. The cuts are labeled by white lines. (b-d) ARPES E - k intensity maps showing the band dispersions of BaK ($x \sim 0.7$) at $T \sim 7$ K taken along cut5 in panel (a) using different polarization directions of the incident Laser (c, v and h). The corresponding MDC (white curves) are shown in top of panels (c) and (d) with their Lorentzian fitting (solid black curves). The white arrows represent the k_F points determined from the MDC peak positions. (e-g) The symmetrized EDCs corresponding to several cuts taken on the FS contour (panel a). (e), (f) and (g) correspond to the inner α , middle β and outer γ bands respectively. The black solid lines represent the EDCs fitting to the BCS function (refer to text).

The FS map of heavily OD BaK ($x \sim 0.7$) taken at low temperature (~ 7 K) is displayed in Fig. 1(a). Three FS sheets could be resolved around the BZ center as expected by band-structure calculations [26, 27]. This is confirmed by the polarization-dependent E - k plots and the corresponding momentum distribution curves (MDCs) at E_F shown in panels (b-d) which correspond to cut5 in panel (a). Only the inner hole-like band (α) appears clearly with v -polarization [panel (c)] while the middle (β) and outer (γ) bands are better observed with h -polarization [panel (d)]. This is an experimental demonstration of the multi-orbital character of the near- E_F bands in BaK. We have carried out a detailed polarization-dependent study [28] and by following the selection rules [29, 30], we could assign the orbital character of the hole bands around the BZ center as follows: The outer band has mainly XZ - Y^2 orbital character, the middle band has XZ/YZ ($+Z^2$) orbital character and the

inner band is mainly characterized with XZ/YZ character. X and Y refer to the tetragonal unit cell axes oriented 45 degrees with respect to the Fe-Fe bond direction and Z is normal to the XY plane.

The energy distribution curves (EDCs) corresponding to the cuts shown in panel (a) and representing the inner, middle and outer bands are respectively displayed in panels (e-g) of Fig. 1. These EDCs, as those in the rest of the paper, correspond to a thin momentum window integrated around k_F points. A common method to check the opening of the SC gap is the symmetrization of the EDCs [31] as we have done here. With symmetrization, it became clear that the SC gap opens for all the cuts taken on the inner and middle FS sheets, where a dip is observed (panels e and f). However, the symmetrized EDCs of the outer FS sheet show a peak (panel g) implying that the SC gap size is negligibly small for all the cuts taken here (panel a). Actually, this is already clear from the E - k plots of Fig. 1 where the inner and middle bands show bending, a typical indication of the SC gap opening while no similar features can be observed in the outer band which crosses E_F . Moreover, we have extracted the SC gap size precisely on the inner and middle FS sheets by fitting their EDCs with a BCS spectral function (similar to ref [15]) and the fitting curves are shown by black solid lines.

In order to get a deeper insight into the evolution of the SC gap size and symmetry in BaK compound, we show in Fig. 2 the ARPES data of samples with different doping levels both in the UD and OD regimes. The upper panel displays the E - k plots corresponding to a cut taken along or close to the high-symmetry line (refer to Fig. 1) and measured in the SC state at $T \sim 7$ K where the SC gap clearly opens. The EDCs corresponding to these E - k plots are shown in panels a, b and c for the inner, middle and outer bands respectively while their symmetrized counterparts are displayed in panels d, e and f. The symmetrized EDCs suggest that, for all dopings, the SC gap opens on all the bands by showing a dip, except on the outer bands of the heavily OD samples ($x \sim 0.6$ and 0.7) where a peak is observed (panel f) implying a negligibly small SC gap in this case (practically zero within error bars). We also note that there is a non-dispersive feature that appears in the EDCs as a second peak at high-binding energy ($\sim 10 - 14$ meV) as shown by black bars in panels a and d of Fig. 2. The intensity of this peak is more enhanced in the OP and UD regions compared to the OD region where it quickly disappears and the band dispersion changes to a simple Bogoliubov quasiparticle dispersion. Moreover, we determined the SC gap size precisely by fitting the EDCs to a BCS spectral function and the results are displayed in Fig. 3. It should be noted that although previous ARPES studies on OP BaK [5, 8] have shown signatures of the two-peak feature observed in our data (Fig. 2), they have poorly resolved the SC peak from the higher binding-energy peak and thus overestimated the SC gap size on the hole FS sheets.

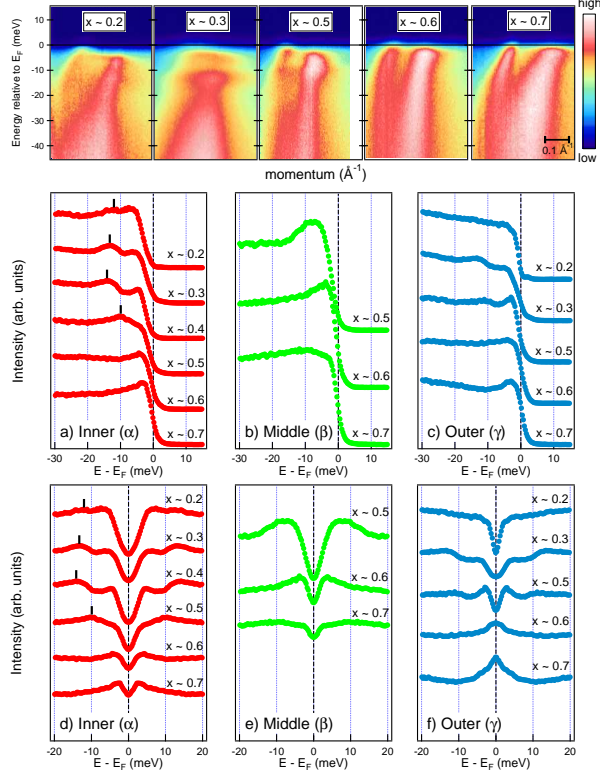


FIG. 2: (color online) Laser ARPES data of BaK with several dopings: E - k plots taken at a cut along or close to the high-symmetry line in momentum space measured in the SC state at low temperature ($T \sim 7$ K) with circularly-polarized light. The energy distribution curves (EDCs) corresponding to these E - k plots where (a), (b) and (c) display the inner, middle and outer band EDCs respectively and their symmetrized counterparts are displayed in panels (d), (e) and (f). The black bars indicate the position of an additional peak observed at higher binding energies compared to the SC peak. The $x=0.4$ data were taken from ref. [15].

It becomes clear from Fig. 3 that by moving away from the OP region, the orbital-independent SC gaps have become strongly orbital dependent. The most striking feature is the abrupt drop in the outer FS sheet gap size in the heavily OD region (for $x \gtrsim 0.6$) while the inner and middle FS gaps roughly scale with T_c . Indeed, this is accompanied by an abrupt change in the FS topology at $x \sim 0.6$ as we show in Fig. 4. Using a He discharge source with $h\nu = 21.218$ eV we show the FS maps of $x \sim 0.5$ and 0.6 in panels a1 and a2 of Fig. 4 respectively with the corresponding magnified images around the X point in panels b1 and b2. The cuts taken near the X point show that while a small electron pocket still exists around the X point in $x \sim 0.5$ (cut c1) similar to OP BaK [32], only hole-like bands reach E_F and form propeller-like FS in $x \sim 0.6$ (cut c2). This can be clearly observed in the magnified E - k plots and their corresponding MDC second derivative plots respectively displayed in panels d1, e1 for cut c1 and panels d2, e2 for cut c2 where an elec-

tron band clearly crosses E_F near the X point for $x \sim 0.5$ but not for $x \sim 0.6$. Also, this is consistent with the observation of an intensity at the X point in panels a1 and b1 ($x \sim 0.5$) but not in panels a2 and b2 ($x \sim 0.6$). Therefore, it can be concluded that the collapse of the outer FS gap to negligibly-small values for $x \gtrsim 0.6$ is probably a consequence of the disappearance of the counter electron pocket at the X point. Such an interpretation is supported by the fact that this gap survives up to $x \sim 0.5$ (Fig. 3) where the electron pockets at the BZ corner still exist.

In an attempt to understand this abrupt change in the gap structure, we illustrate in Fig. 5 the pair scattering process within portions of the FS having similar orbital character (*intra-orbital* interactions). While both $X^2 - Y^2$ and XZ/YZ orbital components exist at the X point around OP BaK (Fig. 5(a)), XZ/YZ rather than $X^2 - Y^2$ orbitals has dominant contribution at this point for the heavily OD case (Fig. 5(b)) as expected by the density functional theory (DFT) calculations [28]. This is consistent with the disappearance of the electron pockets with dominant $X^2 - Y^2$ orbital character for $x \gtrsim 0.6$ as we observed using He-discharge ARPES. On the other hand, the SC gap on the inner and middle hole FS sheets, with dominant XZ/YZ orbital character, has finite values for all doping levels investigated here and roughly scales with T_c (Fig. 3). This may be a consequence of the survival of the inter-band pair scattering related to these sheets through channel (1) (Fig. 5). As for the UD region down to $x \sim 0.2$, the SC gap size at the outer sheet has finite values, unlike the heavily OD case, because the electron pockets exit at the X point and the *intra-orbital* interactions conditions are satisfied.

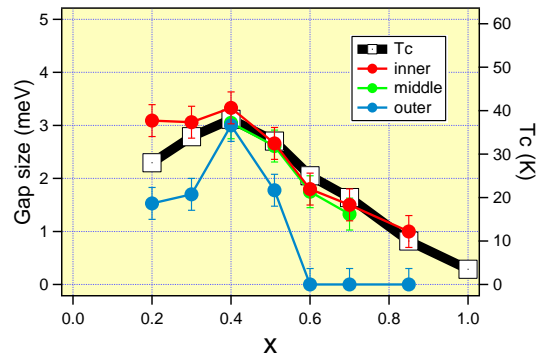


FIG. 3: (color online) Doping dependence of the SC gap size (left y-axis) in BaK compound on the different hole-like bands around the BZ center determined from the data displayed in Fig. 2 and the SC transition temperature T_c (right y-axis). The $x=0.4$ data were taken from ref. [15].

Our results browse the importance of *intra-orbital* interactions for superconductivity in BaK compound and highlight the different roles of $X^2 - Y^2$ and XZ/YZ orbitals as illustrated in Fig. 5. Obviously, we observe a diminishing role of the $X^2 - Y^2$ compared to the XZ/YZ

orbital components in the OD region of BaK. This is in contrast with the OP case where orbital-independent SC gaps were observed [15]. Indeed, the recent INS results on BaK [33] are in agreement with our ARPES results. The magnetic excitation observed by INS is dominated by contributions from the $X^2 - Y^2$ orbital component [34] and its collapse in heavily OD BaK indicate the diminishing role of $X^2 - Y^2$ in this doping regime. Moreover, such an abrupt change at the OD side is expected to have clear implications on the thermodynamic properties, specifically the thermal conductivity and specific heat in OD BaK compared to the OP case.

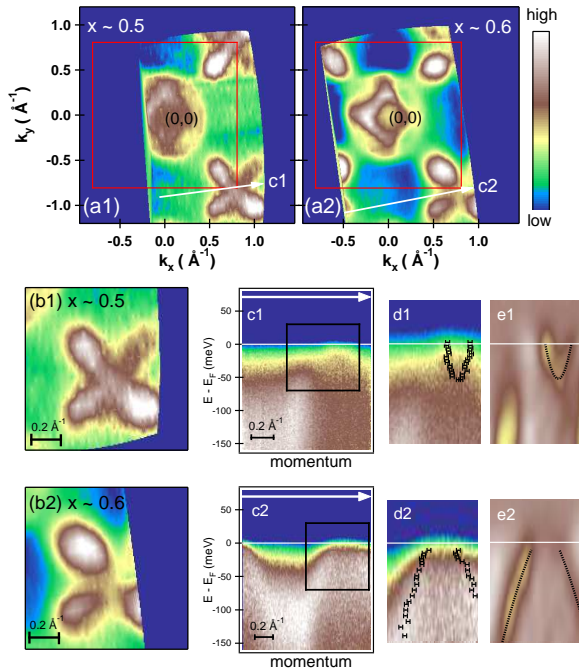


FIG. 4: (color online) FS maps of BaK with $x \sim 0.5$ (a1) and 0.6 (a2) together with the corresponding magnified images around the X point in panels b1 and b2. These maps were taken by He-discharge source with $h\nu = 21.218$ eV at $T \sim 7$ K. The red solid lines enclose the first Brillouin zone. (c1, c2) E - k plots corresponding to cuts taken near the X point and represented by white arrows (c1 at $T \sim 35$ K for $x \sim 0.5$ and c2 at $T \sim 7$ K for $x \sim 0.6$). Magnified E - k plots and MDC second derivative plots corresponding to the windows enclosed by black lines are respectively shown in panels d1, e1 for cut c1 ($x \sim 0.5$) and in panels d2, e2 for cut c2 ($x \sim 0.6$). The dots indicate the MDC peak positions determined from Lorentzian fitting and the black dotted lines are guides to the eye.

The robustness of the outer FS negligible gap with increasing the doping for $x \gtrsim 0.6$ suggests that what we observe here is different from the accidental nodes expected by theoretical studies based on the spin-fluctuation (SF) scenario [4, 16, 21]. Moreover, such a collapse in the outer FS gap may not be easily reproduced by the Random

Phase Approximation (RPA) calculations. Therefore, it may be that other factors like electron correlations effect should be included in these calculations or theoretical calculations beyond the RPA should be considered to account for our experimental results. Also, it may be thought that the similar SC gap size on the inner and middle FS sheets with dominant XZ/YZ orbital character is remnant of the contribution of orbital fluctuations (OF) which are believed to be active in the OP region of BaK [15], but obviously the OF has no contribution to the outer FS sheet in the heavily OD region otherwise its gap would not have collapsed to negligible values. Irrespective of the interpretation, our results show new aspects of the SC gap of BaK compared to previous ARPES reports [7] and can be hardly completely explained by the available theories of iron pnictides which remain to clarify the degree of contributions of SF and/or OF in future studies.

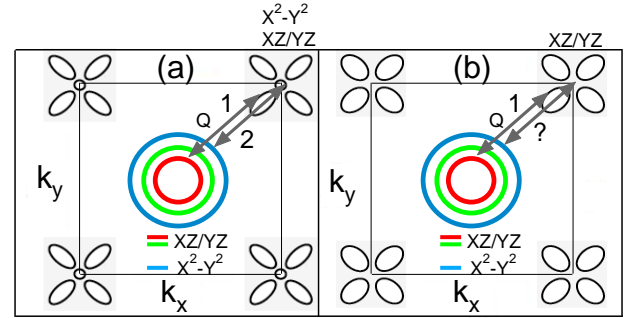


FIG. 5: (color online) Schematics of BaK FSs with the possible *intra-orbital* interaction channels 1 and 2 between the disconnected sheets through the wave vector Q corresponding to BaK with $x \lesssim 0.5$ (a) and $x \gtrsim 0.6$ (b).

In summary, we have precisely determined the doping evolution of the SC gaps on the hole FS sheets around the BZ center in BaK compound after assigning the orbital character of each of these sheets. Unlike the inner and middle FS gaps which roughly scale with T_c , the outer hole FS gap shows an abrupt drop with overdoping (for $x \gtrsim 0.6$) accompanied by the simultaneous disappearance of the electron FS sheet with similar orbital character at the BZ corner. These results browse the different contributions of $X^2 - Y^2$ and XZ/YZ orbitals to superconductivity in BaK and can be hardly completely reproduced by the available theories on iron-based superconductors.

-
- [1] Y. Kamihara *et al.*, J. Am. Chem. Soc. **130**, 3296 (2008).
 - [2] I.I. Mazin *et al.*, Phys. Rev. Lett. **101**, 057003 (2008).
 - [3] K. Kuroki *et al.*, Phys. Rev. Lett. **101**, 087004 (2008).
 - [4] K. Kuroki *et al.*, Phys. Rev. B **79**, 224511 (2009).
 - [5] H. Ding *et al.*, Euro. Phys. Lett. **83**, 47001 (2008).
 - [6] D.V. Evtushinsky *et al.*, Phys. Rev. B **79**, 054517 (2009).
 - [7] K. Nakayama *et al.*, Phys. Rev. B **83**, 020501(R) (2011).
 - [8] D.V. Evtushinsky *et al.*, arXiv1106.4584.
 - [9] T. Hanaguri *et al.*, Science **328**, 474 (2010).
 - [10] A. D. Christianson *et al.*, Nature **456**, 930 (2008).
 - [11] M. Hiraishi *et al.*, J. Phys. Soc. Jpn. **78**, 023710 (2009).
 - [12] H. Kontani *et al.*, Phys. Rev. Lett. **104**, 157001 (2010).
 - [13] T. Saito *et al.*, Phys. Rev. B **82**, 144510 (2010).
 - [14] Y. Yanagi *et al.*, J. Phys. Soc. Jpn. **79**, 123707 (2010).
 - [15] T. Shimojima *et al.*, Science **332**, 564 (2011).
 - [16] K. Suzuki *et al.*, J. Phys. Soc. Jpn. **80**, 013710 (2011).
 - [17] K. Hashimoto *et al.*, Phys. Rev. B **81**, 220501(R) (2010).
 - [18] Y. Nakai *et al.*, Phys. Rev. B **81**, 020503R (2010).
 - [19] H. Fukazawa *et al.*, J. Phys. Soc. Jpn. **78**, 083712 (2009).
 - [20] K. Hashimoto *et al.*, Phys. Rev. B **82**, 014526 (2010).
 - [21] K. Suzuki *et al.*, Phys. Rev. B **84**, 144514 (2011).
 - [22] J.-Ph. Reid *et al.*, Phys. Rev. B **82**, 064501 (2010).
 - [23] K. Ohgushi *et al.*, Phys. Rev. B **85**, 064522 (2012).
 - [24] K. Kihou *et al.*, J. Phys. Soc. Jpn. **79**, 124713 (2010).
 - [25] T. Kiss *et al.*, Rev. Sci. Instrum. **79**, 023106 (2008).
 - [26] S. Graser *et al.*, Phys. Rev. B **81**, 214503 (2010).
 - [27] Z. P. Yin *et al.*, Nat. Mat. **10**, 932 (2011).
 - [28] See Supplemental Material
 - [29] A. Damascelli *et al.*, Rev. Mod. Phys. **75**, 473 (2003).
 - [30] Y. Zhang *et al.*, Phys. Rev. B **83**, 054510 (2011).
 - [31] M.R. Norman *et al.*, Nature **392**, 157 (1998).
 - [32] V.B. Zabolotnyy *et al.*, Nature **457**, 569 (2009).
 - [33] J.-P. Castellán *et al.*, Phys. Rev. Lett. **107**, 177003 (2011).
 - [34] E. Kaneshita *et al.*, Phys. Rev. B **84**, 020511 (2011).

Acknowledgements

We thank Y. Matsuda, T. Shibauchi, S. Kasahara, K. Hashimoto, K. Kontani, K. Kuroki, R. Arita, S. Shamoto, M. Ishikado, T. Kondo, T. Yoshida, S. Ideta and A. Fujimori for informative discussions and Y. Kotani, K. Koizumi and T. Yamamoto for experimental support. This research is supported by the Japan Society for the Promotion of Science (JSPS) through its Funding Program for World-Leading Innovation R and D on Science and Technology (FIRST) program.

Supplemental material

I. ORBITAL CHARACTER OF THE HOLE-LIKE BANDS

In order to determine the orbital character of the hole-like bands around the BZ center, we have considered two different geometries: cut (A) and cut (B) rotated by 45 degrees w.r.t each others as shown in Fig. S1. For cut (A): $X^2 - Y^2$, Z^2 and XZ orbitals have even parities w.r.t the mirror plane while XY and YZ orbitals have odd parities. For cut (B): $X^2 - Y^2$ has odd parity while Z^2 and XY orbitals have even parities. As a result, we conclude the following: $X^2 - Y^2$ has even parity w.r.t cut (A) and odd parity w.r.t cut (B). $XZ/YZ(+Z^2)$ has even parity w.r.t both cuts (A) and (B). XZ/YZ has odd parity w.r.t both cuts (A) and (B). For both cases (cuts (A) and (B)) we used two polarization directions of the incident light: h and v , which respectively correspond to the horizontal and vertical directions as indicated in Fig. S1. The h -polarized light has only an even component w.r.t the mirror plane, however both odd and even components are included in the v -polarized light.

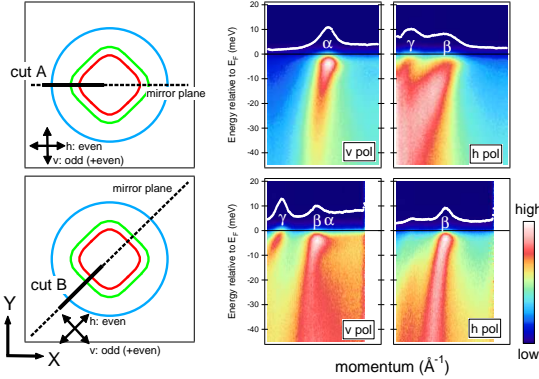


FIG. S1: Polarization-dependent Laser ARPES data of BaK with $x \sim 0.6$: The E - k plots corresponding to cuts A and B taken at different polarization directions are displayed in the upper and lower panels respectively. The inner, middle and outer bands are respectively labeled α , β and γ . The white curves represent the corresponding MDCs at E_F . The directions of cuts A and B (black solid lines) which also represent the analyzer slit direction are illustrated in the left-hand side panels together with the FS contours and the polarization direction of the incident light.

In cut (A), the outer hole band could be clearly observed using h -polarized rather than v -polarized light. However, in cut (B) the opposite is true. Therefore, the dominant orbital component of the outer hole band is $X^2 - Y^2$. The middle band could be observed for both cuts (A) and (B) using h -polarized light which implies that it has $XZ/YZ(+Z^2)$ orbital character. Finally the inner band could be observed for both cuts (A) and (B) using v -polarized light which implies that it has XZ/YZ orbital character.

II. DOMINANT CONTRIBUTIONS OF $X^2 - Y^2$ AND XZ/YZ ORBITALS EXPECTED FROM DFT CALCULATIONS

We performed density functional theory (DFT) calculations to compare the orbital character of the FS sheets at the X point in the UD and OD regions of BaK. The results are displayed in Fig. S2 which show three-dimensional FSs of KFe_2As_2 (c, d) and UD BaK (a, b) obtained by shifting E_F towards higher positions due to the reduction in hole doping. It should be noted that the FSs of heavily OD BaK are similar to those of KFe_2As_2 . These plots were obtained by using the Wien2k code [1] with experimental lattice parameters [2]. Color on the FS sheets depict orbital weights calculated by the Wannier90 [3] via the Wien2Wannier interface [4].

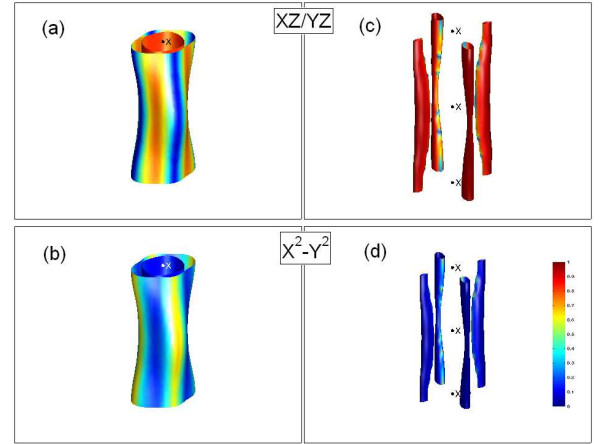


FIG. S2: Three-dimensional Fermi surfaces of KFe_2As_2 obtained from DFT calculations browsing the contribution of $X^2 - Y^2$ and XZ/YZ orbitals to the Fermi surfaces at X point. Panels a and b correspond to UD BaK obtained by shifting E_F towards higher positions.

First we notice a difference in the FS topology between UD (a, b) and KFe_2As_2 (c, d) cases where the FS at the X point has changed from nearly-elliptical-like in the UD region to propeller-like in the heavily OD region and KFe_2As_2 . Moreover, the dominant orbital characters on each FS sheet are browsed by the corresponding colors. While both $X^2 - Y^2$ and XZ/YZ orbital characters have considerable contributions at the X point in the UD and nearly-OP regions (a, b), the XZ/YZ orbital character becomes dominant at that point in the OD region (c, d).

-
- [1] P. Blaha *et al.*, *WIEN2K, An Augmented Plane Wave + Local Orbitals Program for Calculating Crystal Properties* (Karlheinz Schwarz, Tech. Universität Wien, Austria, 2001).
 - [2] M. Rotter *et al.*, *Angew. Chem. Int. Ed.* **47**, 7949 (2008).
 - [3] A. Mostofi *et al.*, *Comput. Phys. Commun.* **178**, 685 (2008).
 - [4] J. Kune *et al.*, *Comput. Phys. Commun.* **181**, 1888 (2010).